What distinguishes 100-year precipitation extremes over Central European river catchments from more moderate extreme events?

Florian Ruff and Stephan Pfahl

Freie Universität Berlin, Institute of Meteorology, Carl-Heinrich-Becker-Weg 6-10, 12165 Berlin, Germany
Correspondence: Florian Ruff (florian.ruff@met.fu-berlin.de)

Abstract. Historical extreme flooding events in Central European river catchments caused high socioeconomic impacts. Previous studies analysed single events in detail but did not focus on a robust analysis of the underlying extreme precipitation events in general as historical events are too rare for a robust assessment of their generic dynamical causes. This study tries to fill this gap by analysing a set of realistic daily 100-year large-scale precipitation events over five major European river catchments with the help of operational ensemble prediction data from the ECMWF. The dynamical conditions during such extreme events are investigated and compared to those of more moderate extreme events (20- to 50-year). 100-year precipitation events are generally associated with an upper-level cut-off low over Central Europe in combination with a surface cyclone southeast of the specific river catchment. The 24 hours before the event are decisive for the exact location of this surface cyclone, depending on the location and velocity of the upper-level low over Western Europe. The difference between 100-year and more moderate extreme events vary from catchment to catchment. Dynamical mechanisms such as an intensified upper-level cut-off low and surface cyclone are the main drivers distinguishing 100-year events in the Oder and Danube catchments, whereas thermodynamic mechanisms such as a higher moisture supply in the lower troposphere east of the specific river catchment are more relevant in the Elbe and Rhine catchments. For the Weser/Ems catchment, differences appear in both dynamical and thermodynamic mechanisms.

1 Introduction

Flooding events in highly populated areas are one of the main natural hazards for the modern society (Hammond et al., 2015; Kreibich et al., 2014; Barredo, 2007). Central Europe was regularly affected by substantial flooding events in the last decades in several river catchments due to extreme precipitation events. Remarkable flooding events were the Rhine floods in June 2021 and in December 1993, the Oder floods in May 2010 and in July/August 1997, the Elbe flood in March/April 2006 as well as the flooding events in Central Europe in June 2013 and in August 2002, where several catchments, but mainly the Danube and Elbe, were effected. All these events had devastating impacts such as several to hundreds of human life losses, thousands of evacuations as well as economic losses of several million to billion euros (Munich RE, 2022; Engel, 2004; Re, 1999). The Central European flood in August 2002 was the most expensive natural hazard for Central Europe, caused accumulated costs of about 15 billion euros for both public and private properties and even impacted business interruptions after the event (Mueller, 2003), while the Rhine flood in June 2021 was globally the second most expensive natural hazard in

2021 (Statista, 2022). These damages were associated with high water levels, partly even the highest water levels on record. For instance, during the Central European flood in June 2013, several gauges measured record water levels including the German city Dresden where the highest water levels of about 12.75 m were recorded since 1501 (Merz et al., 2014). However, several improvements in flood risk management implemented in the beginning of the 21th century following the floods at the

30 end of the 20th century prevented some areas from socioeconomic losses to extend that occurred earlier (Merz et al., 2014; Bissolli et al., 2011). Nevertheless, as losses can never be totally eliminated, it is important to gain more knowledge about the atmospheric triggering mechanisms that induce such extreme floods to improve forecasts of these events and warn the public at an early stage. Additionally, flooding events can become even more relevant in the future as climate simulations show a higher frequency of extreme precipitation events in the mid-latitudes in a warmer climate (Pendergrass and Hartmann, 2014; Fischer

35 et al., 2013; O'Gorman and Schneider, 2009).

Central European flooding is typically associated with large-scale extreme precipitation events over a river catchment, which are linked to mid-latitude cyclones that become quasi-stationary over Central or Eastern Europe for a few days as described in Grams et al. (2014); Pfahl (2014); Blöschl et al. (2013); Bissolli et al. (2011); Ulbrich et al. (2003). In case studies, Grams et al. (2014) and Ulbrich et al. (2003) found that the origin of such a circulation anomaly was linked to upper-level Rossby wave

40 breaking and the formation of an upper-level cut-off low over Western Europe. The stationarity of such a cut-off low can be facilitated by a blocking anticyclone over the North Atlantic, sometimes in combination with a blocking over Western Russia as shown by Blöschl et al. (2013). Such an upper-tropospheric configuration is often associated with either a surface cyclone moving from Western Europe southeastwards around the southern flanks of the Alps, or cyclogenesis over the Ligurian Sea, followed by a northeastward track of the cyclone towards Central or Eastern Europe (Bissolli et al., 2011; Mudelsee et al.,

45 2004; Ulbrich et al., 2003). Such cyclone tracks are typically known as a "Vb" weather type (van Bebber, 1891). However, the Central European flood in June 2013 was triggered by surface cyclones that formed over Eastern Europe but moved towards Central Europe as well (Grams et al., 2014). Although a surface cyclone is often of high relevance for producing extreme precipitation, it is not necessary that this cyclone is associated with extremely low pressure (Pfahl and Wernli, 2012). This was also shown by Grams et al. (2014), as the surface cyclones during the Central European flood in June 2013 were rather shallow

50 with minimum pressure between 995 hPa and 1000 hPa. Hence, other important processes such as the transport of atmospheric moisture and the quasi-stationarity of the weather pattern have to be taken into account.

Surface cyclones can facilitate the transport of atmospheric moisture in the lower troposphere towards a certain area. For extreme flooding events, typically several moisture sources are important. On the one hand, moisture can evaporate into the atmosphere from the North Atlantic as well as from the Mediterranean (Blöschl et al., 2013; Sodemann et al., 2009; Ulbrich

55 et al., 2003). On the other hand, a high amount of moisture evaporates over continental areas such as Central and Eastern Europe along the tracks of cyclones (Grams et al., 2014; Winschall et al., 2014). Especially during the northward movement of "Vb" cyclones towards Central or Central Eastern Europe, continental moisture sources become more dominant (Winschall et al., 2014; James et al., 2004). Regional ascent of these moist air masses occurs shortly before and during the extreme precipitation events over the specific river catchment. The orographic effects of the Alps and other mountainous areas additionally play an

60   important role for the location of the extreme precipitation as it was the case in several of the extreme flooding events (Grams et al., 2014; Szalińska et al., 2014; Blöschl et al., 2013; Ulbrich et al., 2003).

However, just the occurrence of an extreme precipitation events does not necessarily trigger a major flood event. As the case studies cited above show, also hydrological preconditions such as an (almost) saturated soil and a high river runoff already prior to the event are important prerequisites for the development of a flooding as well. Such conditions are often the result of
65   the accumulation of precipitation during the days or weeks before the extreme flooding (Grams et al., 2014; Merz et al., 2014; Bissolli et al., 2011; Engel, 1997).

In most previous studies, detailed analyses of the atmospheric dynamics of historical extreme precipitation events associated with Central European flooding were done in case studies. Some of these studies compared their results with a few other floods in the same river catchment. However, due to the shortage of the observational record it is difficult to determine the return
70   level of the most severe historical floods, and there are too few events to systematically investigate the generic atmospheric processes leading to such events. Today's knowledge about the mechanisms of such extreme events is, therefore, based on analyses of single events as well as on statistical investigations of more moderate precipitation events with return periods on the order of one up to a few years (Donat et al., 2013; Sillmann et al., 2013; Pfahl and Wernli, 2012; Kenyon and Hegerl, 2010). Higher return levels are typically estimated based on extreme value theory such as in Maraun et al. (2011). Still, the length of
75   observational time series plays an important role for the precision of such statistical estimates as well. Additionally, a detailed analysis of the underlying meteorological processes is complicated as the extreme events are usually not explicitly identified in such statistical assessments. There is a systematic lack of knowledge on the mechanisms leading to very extreme precipitation events with return periods on the order of 100 years. It is also unclear how these mechanisms of 100-year events distinguish from more moderate precipitation events. These knowledge gaps are addressed in the present study.

80   This study focuses on the dynamical mechanisms behind very extreme large-scale precipitation events with a return period of 100 years in five major Central European river catchments, which have the potential to cause devastating flooding events. In order to robustly analyse these mechanisms, we use data from operational ensemble weather prediction simulations to generate a large set of multiple realisations of possible weather situations for a quasi-stationary climate following Breivik et al. (2013). This set of multiple possible realisations has an equivalent length of 1200 years and, hence, is several times longer
85   than conventional observational time series. Several extreme precipitation events with return periods of at least 100 years are identified in this data set with the help of extreme value theory. Estimates of such extreme return levels from observational time series are compared with the ensemble prediction data to evaluate the realistic representation of extreme precipitation magnitudes. The atmospheric processes associated with the 100-year events are then systematically analysed. In a second step, the results are compared to the conditions during more moderate extreme precipitation events.

90   The following section 2 describes the ensemble prediction data set that is used for the identification and meteorological analysis of 100-year precipitation events. In addition, three observational data sets are introduced that are used for verification. All methodological aspects regarding the processing of ensemble data and further statistical methods are explained in section 3. In section 4, both the atmospheric processes associated with 100-year events and the differences to less extreme precipitation

events as well as an analysis of tracks, frequencies and intensities of objectively identified surface cyclones during the extreme
95   events are presented. Finally, conclusions and a discussion of our most important findings are provided in section 5.

2   Data

For this study, a large data set of daily precipitation events is constructed from operational ensemble weather prediction data.
Additional observational data are used to evaluate this model-based data set. All these data sets are described in the following.

2.1   Ensemble prediction data

100   The archive of the operational weather prediction model of the Integrated Forecasting System, provided by the European
Center for Medium-Range Weather Forecasts (ECMWF), is used to get a large set of simulated but realistic daily weather
and precipitation events from their ensemble prediction system (EPS). The workflow of the EPS is described in more detail
in Molteni et al. (1996). On every day, ensemble simulations are started with lead times of at least 10 days and 51 ensemble
members. One member represents the control run with no perturbed initial conditions while the other 50 member represent
105   perturbed runs with slightly changed initial conditions between each ensemble member and additional stochastic perturbations
introduced during the model integration. Since the 25th of March 2003, these ensemble simulations are operated two times a
day, starting at 0 and 12 UTC. The combination of 51 ensemble members and two daily initialisations results in 102 simulations
per real day. The basis for this study are daily precipitation sums from these forecasts computed by adding up the large-scale
and convective precipitation over 24 hour time periods contiguously.

110   Instead of the daily precipitation sums for all 10 days of each simulation, just the 10th day of each simulation (accumulated
precipitation between forecast hour 216 and forecast hour 240, resulting in a 24-hour time period each) is used in this study,
following Breivik et al. (2013). They used a large data set from ensemble simulations to estimate return values of wave heights
over the oceans. To this end, Breivik et al. (2013) assumed that the weather conditions, and especially the wave heights, of the
10th day of each simulation are independent between the different ensemble members due to the advanced lead time. During
115   the first days, the simulations of the different member are correlated due to a strong dependency on the initial conditions, but
this correlation weakens when the forecasts advance in time. Breivik et al. (2013) also performed several statistical evaluations
to demonstrate this independence on the 10th forecast day and to evaluate the statistics of the simulated wave heights in
comparison to observations. Also for the daily precipitation events investigated in this study, due to the high spatial and
temporal variability of precipitation, we assume that the weather conditions of each 10th simulation day do not strongly
120   correlate with the initial conditions of the simulations and the daily precipitation events can thus be regarded as independent
realisations. Following Breivik et al. (2013), this assumptions is evaluated statistically as described in section 3.2.

First tests showed that very high percentiles (99th, 99.9th and 99.99th), which represent the most extreme precipitation events
of this daily data set, are systematically higher for the first years of the ensemble prediction data (see Supplementary Fig. S1
for the Danube catchment). Since 2008, the data show a more consistent amplitude of these different percentiles, comparable to
125   the observational data sets (not shown). Hence, to exclude any possible inconsistencies due to temporal inhomogeneity of the

data, just the ensemble prediction data from the 1st of January 2008 until the 31th December 2019 are used in the following. The combination of 102 different simulated precipitation events per real day and 12 years of simulations from the archive of the EPS leads to an overall data set of 1224 years of simulated but realistic daily precipitation events. The data cover the entire globe and are available on a regular lon/lat grid, whose resolution changes over time due to updates of the model system. Since

130 these precipitation data are further used to compute daily precipitation sums for large Central European river catchments (see section 3), they are first interpolated on a relatively coarse grid of 1°x 1°.

To study the atmospheric conditions during and before the most extreme daily precipitation events, several additional meteorological parameters are extracted from simulations that included an extreme precipitation event (as defined below) and used for composite and single event analyses during and up to four days ahead of the events. All parameters are available every six

135 hours from forecast hour 120 (4 days before the event occurred) until forecast hour 240 (the end of the event) on a regular lon/lat grid with a spatial resolution of 0.1°x 0.1°. These data cover a large European region, ranging from 30°W to 45°E and from 25°N to 75°N.

2.2   Observational data sets

Three observational precipitation data sets (REGEN, HYRAS and E-OBS) are used to evaluate the precipitation climatologies

140 obtained from the ensemble simulations. These data sets are all based on station observations and mainly differ in their spatial resolution, region of coverage and method used for the interpolation of available station data to a regular spatial grid.

2.2.1   REGEN data

The Rainfall Estimates on a Gridded Network (REGEN) data set (Contractor et al., 2020) is a observational precipitation data set covering global land areas. It is based on the spatial interpolation of in situ surface precipitation measurements from

145 several large observational archives, such as the Global Historical Climate Network Daily, hosted by the National Oceanic and Atmospheric Administration, and the Global Precipitation Climatology Centre, hosted by Deutscher Wetterdienst. All observed precipitation time series are quality controlled before interpolation. The station density differs strongly between specific regions and continents. Africa and Central Asia have a low density of stations while many parts of North America, Australia and especially Europe have a high density. Besides daily precipitation sums, this data set provides parameters like

150 the standard deviation of these precipitation sums as well as the number of rain gauges within each grid box. For this study, just the daily precipitation sums of Version 1-2019 based on around 135.000 stations are used for further investigations. These data are available on a regular lon/lat grid for all global land areas with a spatial resolution of 1°x 1° from the 1st of January 1950 until the 31th of December 2016.

2.2.2   HYRAS data

155 The HYRAS data set represents a climatology of daily precipitation sums for Germany and river catchments of major rivers in neighbouring countries, provided by Deutscher Wetterdienst (DWD). This data set is based on thousands of in situ observations.

The number of stations increases over time, and the station density differs between countries and is much higher in Germany and the Netherlands compared to parts of, e. g., Poland and France. All these observational station data were quality controlled by the DWD and were interpolated to a Lambert Conformal Conic Projection by using the REGNIE method, which is described in more detail in Rauthe et al. (2013). Here, these data are interpolated again on a regular lon/lat grid with a spatial resolution of 0.05°x 0.05°. They are available from the 1st of January 1951 until the 31th December 2015 and cover an area of Germany and adjacent river catchments ranging from about 1.85°E to 20.80°E and 45.10°N to 55.65°N.

2.2.3 E-OBS data

The E-OBS data set is an on-going observational data set for European land areas, provided by the European Climate Assessment & Dataset (ECAD) initiative. This data set combines observational data from a large set of stations across several countries, provided by National Meteorological Services, in an ensemble approach with 100 ensemble members for several meteorological parameters such as temperature and precipitation, as described in Cornes et al. (2018). The observational data are quality controlled, both by each National Meteorological Service and by the ECAD itself. As for the other data sets, the temporal and especially the spatial availability of station data differs, especially across national borders, with higher densities in Central and Northern Europe. Through the ensemble simulations, the uncertainties of the interpolation of the data to a regular grid is reduced. For this study, just the daily precipitation sums are used. Based on E-OBS version 21.0e, these precipitation data are available on a regular lon/lat grid with a spatial resolution of 0.1°x 0.1° from the 1st of January 1950 until the 31th of December 2019 and cover a large European region, ranging from 25.0°W to 45.5°E and 25.0°N to 71.5°N.

3 Methodology

In this section, the methodology to identify and analyse extreme precipitation events in ensemble prediction data is described, starting with the catchment definitions of the selected rivers, followed by the statistical evaluation of the suitability of the ensemble data. Afterwards, the determination of the extreme events is introduced as well as the composite analysis and cyclone identification and tracking method that are used for characterising the underlying atmospheric processes.

For simplicity, all figures and analyses in section 3.2 are only shown for the Danube river catchment as representative for all catchments. In case that results for other catchments differ substantially from those of the Danube catchment, this is mentioned in the text.

3.1 River catchments

Five major Central European river catchments are considered in this study. Four river catchments represent the rivers Rhine, Elbe, Oder and Danube while the fifth catchment covers the region of the two rivers Weser and Ems in Northern Germany, here denoted as Weser/Ems. As explained in section 1, flooding events in the past have shown that all these regions are affected by risks of flooding and associated socio-economic impacts during extreme precipitation events.
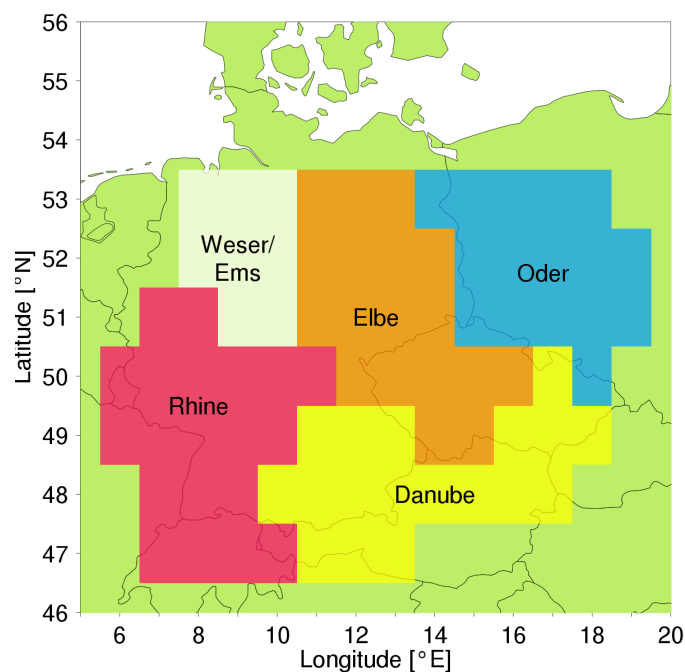
Figure 1. River catchments of the rivers Rhine, Elbe, Oder, Danube and the combination of the rivers Weser and Ems, denoted Weser/Ems, based on a 1°x 1° lon/lat grid over Central Europe.

The spatial coverage of these selected river catchments as adopted in this study is shown in Fig. 1. The spatial resolution of 1°x 1° is due to the resolution of the daily precipitation data of the ensemble prediction data (see section 2.1). Each grid point has been allocated to one of the five river catchments based on a river basin map by the Waterways and Shipping Administra-
190   tion of Germany (Wasserstraßen- und Schifffahrtsverwaltung des Bundes, 2022). Due to the relatively coarse resolution, this does not exactly reproduce the river catchments, but still provides a clear separation of the larger-scale precipitation patterns potentially associated with flooding in the different catchments.

Precipitation time series for each river catchment are constructed by averaging the time series from the associated 1°x 1° grid boxes, both from the ensemble predictions and observational data sets. Only for the comparison with HYRAS data, the
195   methodology is slightly adapted because HYRAS does not cover the entire catchments shown in Fig. 1. Therefore, only 1°x 1° boxes with a HYRAS data coverage of at least 90% are considered in this comparison.

3.2 Statistical evaluation of the ensemble prediction data

In order to evaluate the suitability of the precipitation data set obtained from the ensemble weather prediction data base for the analysis of extreme precipitation events, several statistical properties of the data are considered following Breivik et al.
200   (2013). The following statistical evaluations cover the independence of events between ensemble members as well as within a

specific member and a comparison of the statistical distributions of daily precipitation between the members as well as with observational data. Figure 2 shows the results of these analyses exemplarily for the Danube catchment.

A basic assumption in the application of the ensemble prediction data set as a climatological data basis for our analysis is that the precipitation accumulated over the 10th forecast day is independent between the ensemble members. To statistically

205 evaluate this independence, Fig. 2a shows the statistical distribution of Spearman correlation coefficients between all possible combinations of ensemble members (5151 in total). The left box plot represents the correlations between the entire daily time series of two ensemble members with a total length of 12 years. These correlation coefficients vary between 0.12 to 0.32, with a mean correlation of about 0.19. All correlations are statistically significant, which is also due to the long time series. Physically such relative small correlations between the precipitation time series may arise from low frequency (longer than 10 days)

210 variability in the climate system, which affects all ensemble members from the same initialisation date in a similar manner. However, in order to estimate 100-year return values and identify 100-year precipitation events, in this study we do not use the entire time series, but only the annual maxima of daily precipitation (block maximum approach, see section 3.3). Therefore, the right box plot in Fig. 2a indicates the distribution of correlation coefficients between such annual maximum values (12 values for each ensemble member). Most of the correlation coefficients are around 0 (mean correlation of 0.04), but there is a

215 huge spread between -0.90 and +0.85. In order to estimate the statistical significance in such a situation of multiple correlation coefficients, we apply the False Discovery Rate (FDR) test of Benjamini and Hochberg (1995), as described in Ventura et al. (2004), to the entire sample of p-values associated with the individual correlation coefficients from the various combinations of ensemble members. According to this FDR test, only one out of the 5151 correlation coefficients for the Danube catchment can be considered as significant, and this number of significant correlations varies between zero and two for the other catchments.

220 These very low numbers of significant correlation coefficients, together with the relatively small correlations of the entire time series, justify our assumption of independence, in particular when considering extreme (such as annual maximum) daily precipitation events.

To put the correlation coefficients between the time series into context and also evaluate the auto-correlation of precipitation time series obtained from one ensemble member, Fig. 2b shows the distribution of auto-correlation coefficients for the entire

225 daily precipitation time series and lags between one and five days. For a lag of one day, the mean correlation is 0.10, which is a bit lower, but still in the same range as the mean correlation of time series from different ensemble members. Also this small auto-correlation can result from low-frequency variability of the climate system that affects both initial conditions of the forecasts that are initialised one day after the other. For lags of two days and more, the auto-correlation rapidly decreases, with a mean correlation of 0.04 for a lag of five days.

230 A second important criterion for the applicability of the ensemble weather prediction data to analyse extreme precipitation events is a realistic representation of observed precipitation statistics. This is evaluated by comparing quantiles from the statistical distributions of daily precipitation between the ensemble data (taking all members together) and three observational data sets (REGEN, HYRAS and E-OBS) in quantile-quantile plots (QQ-plots), as shown in Fig. 2c. A perfect match of the distributions would be indicated by quantiles falling on the diagonal. This is the case for precipitation intensities below about 20 mm,
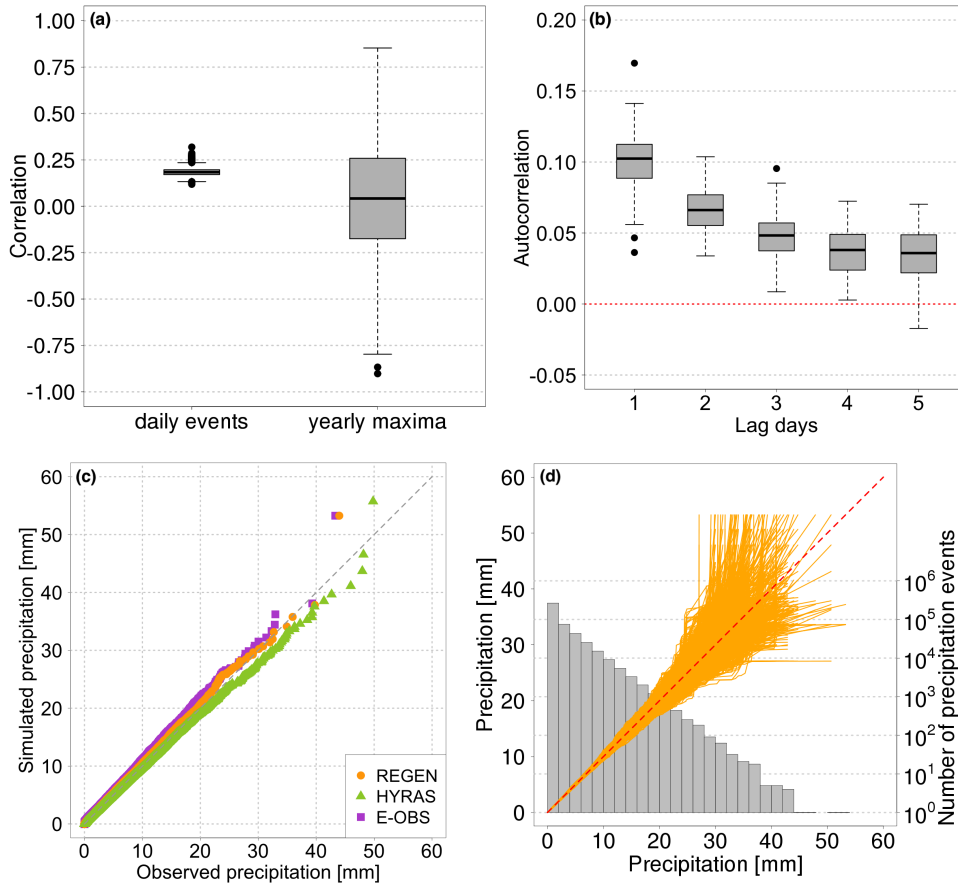
Figure 2. Statistical evaluation of daily precipitation data obtained from ensemble weather predictions for the Danube catchment. **(a)** Distribution of Spearman correlation coefficients between (left) daily precipitation time series and (right) annual maximum daily precipitation values for every combination of ensemble members (5151 in total). The box is bordered by the 25th and 75th percentile, while the whiskers extend to the most outer point which is not more than 1.5 times the interquartile range from the box. **(b)** Distributions of temporal autocorrelation coefficients of every ensemble member daily precipitation time series (102 in total) for lags of one to five days. **(c)** Quantile-quantile-plot of daily precipitation from the ensemble weather prediction data (vertical axis) and three observational data sets (REGEN, HYRAS and E-OBS; horizontal axis). **(d)** Quantile-quantile-plot of daily precipitation from every ensemble member combination (5151 in total). Grey bars indicate the intensity distribution from the entire ensemble prediction data set.

235 which occur most frequently (see Fig. 2d). In this range, the distributions of daily precipitation from the ensemble data and the three observational data sets are thus almost equal. For higher intensities, there are some differences between the quantiles, with the ensemble data overestimating the higher quantiles compared to E-OBS data, but underestimating them in comparison to HYRAS. The deviations from the diagonal are mostly smaller in other catchment areas (see Supplementary Fig. S2), which may be related to the relatively complex topography of the Danube catchments and the limited spatial resolution of both model

240 and observational data. All together, this analysis shows that the ensemble weather prediction data set represents the statisti-

cal distribution of daily precipitation reasonably well and lies within the observational uncertainties (differences between the observational data sets) even for high quantiles corresponding to extreme precipitation events.

Finally, the statistical distributions of daily precipitation are also compared between the individual ensemble members. Figure 2d shows the QQ-plots for every possible combination of ensemble members (5151 in total), each one as an orange line. The grey bars show the precipitation distribution of all daily events from all ensemble members. All QQ-plots show nearly identical distributions for all members and low precipitation intensities (20 mm and lower). For higher precipitation intensities, the QQ-plots start to diverge. Such a divergence is expected since the time series are 12 years long and a daily precipitation event of 30 mm roughly corresponds to a 10-year event. Random fluctuations in the occurrence of such rare events can thus lead to large differences in the higher quantiles between the members.

In conclusion, the analyses in this section have shown that the ECMWF ensemble prediction systems produces realistic statistical distributions of daily precipitation in the selected catchments and that extreme precipitation events obtained from the ensemble prediction data set can be considered as statistically independent. The data set is thus suitable for a systematic analysis of very extreme, 100-year precipitation events.

3.3 Determination of extreme precipitation events

Building on the statistical evaluation presented in section 3.2, we now pool the daily precipitation data from all ensemble members together. To determine return levels corresponding to 100-year (and also 20- and 50-year) return periods and select the corresponding precipitation events, the block maximum approach from extreme value statistics is applied (see Coles et al., 2001). A yearly period is selected to determine block maxima, resulting in 1224 block maxima in total. Such a yearly block size is large enough to fulfil the Fisher-Tippett theorem, such that a generalised extreme value distribution (GEV) can be fitted to the block maxima. Three parameters, the location (μ), scale (σ) and shape (ξ) parameter are estimated to obtain the best fit of the extreme value distribution as it can be seen in Supplementary Fig. S3 for the Danube catchment. From these three parameters, the return level l can be computed by the following equation:

$$
\begin{aligned}
l &= \mu + \sigma \cdot \frac{(x^{\xi} - 1)}{\xi} \\
x &= \frac{-1}{log(1 - \frac{1}{p})}
\end{aligned}
\tag{1}
$$

where a specific return period in years is denoted by p following Stephenson (2002). Confidence intervals of the return level are obtained from bootstrap resampling (see Coles et al., 2001). A new set of block maxima is drawn with replacement from the original set and the return level is again obtained from a GEV fit and Eq. (1). This procedure is repeated 1000 times, leading to 1000 different return levels from which the 0.025 and 0.975 quantiles are used as confidence intervals.

Table 1 shows the 100-year return levels and confidence intervals estimated for the different catchment following this proce-
dure. For the explicit analysis of 100-year events, all daily precipitation events in a specific river catchment with a precipitation

Catchments	Return levels	Confidence intervals	
Rhine	34.49 mm	33.28 mm	35.84 mm
Weser/Ems	42.56 mm	39.80 mm	45.32 mm
Elbe	36.62 mm	34.78 mm	38.75 mm
Oder	38.58 mm	36.87 mm	40.50 mm
Danube	40.21 mm	38.65 mm	41.92 mm

Table 1. Return levels and confidence intervals for 100-year daily precipitation events in different river catchments, obtained from the procedure in section 3.3.

amount above the 100-year return level are selected. This results in 13 100-year events for the Danube catchment (Rhine: 13, Weser/Ems: 10, Elbe: 11, Oder: 13). For comparison, more moderate extreme precipitation events that fall in between the 20-year and 50-year return level are chosen (Danube: 41 events, Rhine: 42, Weser/Ems: 29, Elbe: 38, Oder: 36).

3.4 Composite analysis

275 To analyse the generic meteorological conditions associated with extreme precipitation events, composites are constructed by averaging an atmospheric field from a specific lead time over all events from a given catchment and intensity (100-year or moderate, 20-50-year events). Such a composite analysis emphasises the structures that are common to all or most of the events. In addition, all 100-year events have been examined individually, and specifically noticeable anomalies are mentioned in the text. By averaging fields from a fixed lead time, the composites are representative of a specific time step relative to the 280 occurrence of the daily extreme event, but not of a specific time of the day, as the forecasts have been initialised at both 0 and 12 UTC. Composites of meteorological parameters with a strong diurnal cycle thus have to be interpreted with care. Differences between composite patterns are tested for statistical significance at each grid point using a Student's t-test on a significance level of 0.05 (see Coles et al., 2001).

3.5 Cyclone identification and tracking

285 As precipitation extremes in Europe are know to be linked to the occurrence of mid-latitude cyclones (Pfahl, 2014), the composite analysis is complemented by an automated cyclone identification and tracking method following Wernli and Schwierz (2006) in a slightly updated version as documented in Sprenger et al. (2017). Cyclones are identified and tracked based on 6-hourly sea level pressure (SLP) fields from the ECMWF ensemble forecasts. Cyclone centers are determined as local minima of the SLP, and subsequent cyclone centers are connected to form a cyclone track if they occur within a search area determined 290 by the previous cyclone track.

Here, this algorithm is used to find the surface cyclone that is associated with a specific extreme precipitation event. For each event, all cyclone tracks are considered as possible candidates that exist at least up to six hours after the begin of the 24-hour event. The closest cyclone located in a specific area around the river catchment during that time step (Danube: 10°E-25°E &

40°N-50°N, Rhine: 5°E-20°E & 42°N-52°N, Weser/Ems: 5°E-20°E & 45°N-55°N, Elbe: 10°E-25°E & 45°N-55°N, Oder:

295   15°E-30°E & 45°N-55°N) is then associated with the event. These areas are mainly located southeast of the river catchments, where our composite analysis indicates a SLP minimum (see below). There are a few cases when no cyclone is located in the predefined area, when the SLP field is rather flat and does not possess a well-defined minimum. These cases are excluded from the analysis of cyclone tracks. Additionally, the cyclone tracks associated with the extreme events do not have the same length, such that the number of considered cyclones differs between lead times.

4   Results

In the first part of this section, the temporal and spatial distributions of 100-year and more moderate extreme events are shown (section 4.1). Afterwards, the main results of this study are presented covering the atmospheric conditions associated with 100-year events and their differences to more moderate events (section 4.2). The results of the cyclone identification and tracking approach are then shown for both types of events in section 4.3. For simplicity, the 100-year precipitation events are abbreviated

305   as MEPE (most extreme precipitation events) and the more moderate, 20-50-year events as LEPE (less extreme precipitation events) in this section. Several figures and analyses are only shown for the Danube catchment, but results for other catchments are also discussed, in particular if they are substantially different.

4.1   Spatial and temporal distribution

4.1.1   100-year precipitation events

310   In this section, 100-year events are characterised in terms of their spatial precipitation patterns and time of occurrence. The MEPE are typically associated with high precipitation amounts over the entire river catchment. In most catchments, the composite precipitation patterns have a maximum near the center and a relatively flat decrease of the average daily precipitation towards the boundaries, except for the Danube (see Fig. 3a) and partly the Rhine catchment. There, the highest precipitation rate are found along the northern flank of the Alps, indicating the importance of orographic precipitation enhancement in these

315   two catchments. The composite maximum precipitation amounts are largest for the Weser/Ems and Danube catchments with 52.6 mm and 44.1 mm, respectively, followed by the Oder (42.1 mm), Elbe (40.9 mm) and Rhine (37.6 mm) catchments. The high values in the Weser/Ems region are associated with the relatively small catchment size.

Interesting aspects of 100-year precipitation events are their time of occurrence during the year and their temporal variability during the day of the event. The monthly frequencies of MEPE for all river catchments are presented in Fig. 4a, which clearly

320   shows that such events occur most frequently during the extended summer months June-September. While the frequency over, e.g., the Oder catchment is relatively high in July and August, the events over the Weser/Ems catchment are rather evenly distributed over the warmer months. A few events, for instance over the Rhine catchment, also occur in May or October, which is, however, rather rare.
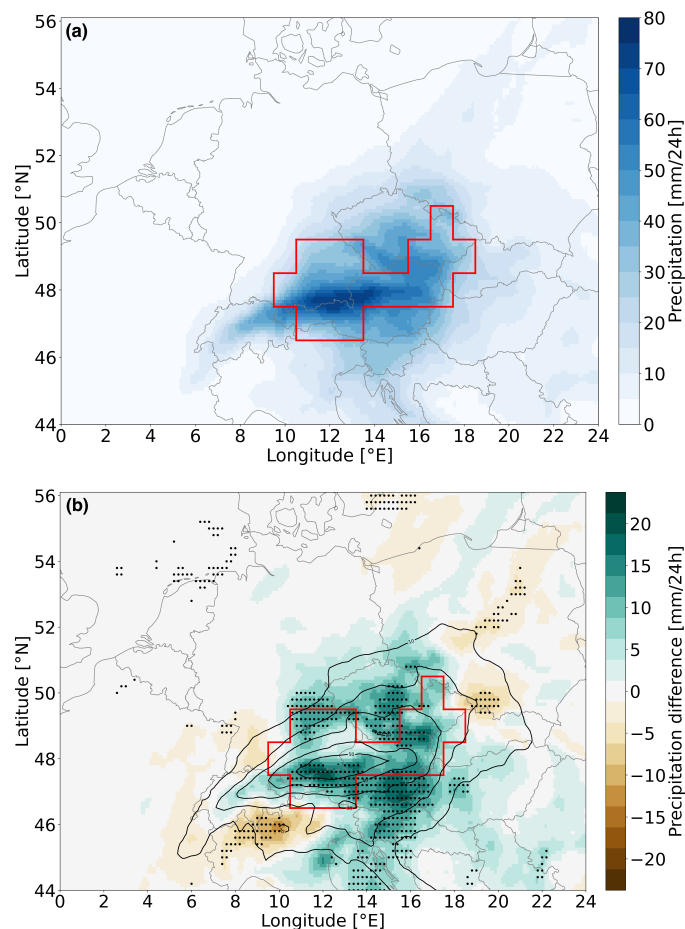
Figure 3. (a) Composite of the accumulated daily precipitation amount during all MEPE. **(b)** Composite difference between the accumulated precipitation amount of MEPE and LEPE. Results are shown for events over the Danube catchment which is indicated by the red line. In **(b)**, positive (negative) values represent higher (lower) precipitation amounts during MEPE, significant differences are marked by a black dot and the LEPE composite is shown as black contours (contour interval of 10 mm).

To quantify the temporal variability of precipitation during the day of the MEPE, the six-hourly precipitation values of each
325 event are ranked by their intensity, starting with the highest intensities, as shown in Supplementary Fig. S4 for the Danube catchment. Large differences between the red boxes would indicate that the daily MEPE are mainly caused by very intense six-hourly precipitation periods, whereas relatively equal distributions would indicate that the MEPE are due to persistent precipitation during the entire day. For the Danube catchment, there is no clear indication that just one of these types dominates. There is some sub-daily variability during the MEPE, with the six-hourly precipitation during the most intense period being
330 about 75% higher than in the weakest period. Similar sub-daily distributions are found for the Rhine and Oder catchments. Just the Weser/Ems and Elbe events show a tendency towards larger differences, that is MEPE events being more influenced by intense six-hourly precipitation.
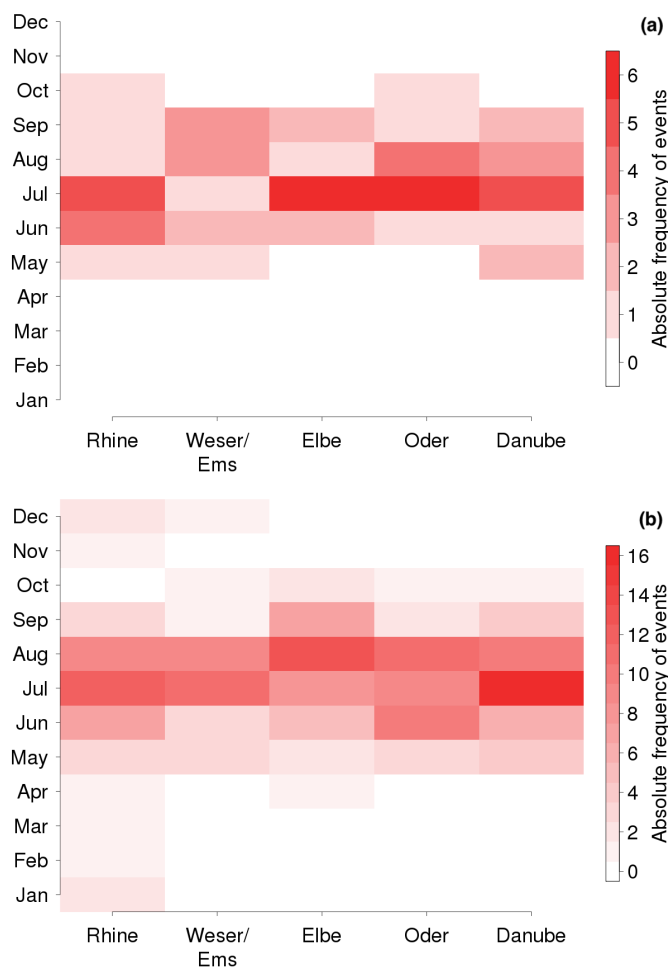
Figure 4. Monthly distribution of **(a)** MEPE and **(b)** LEPE for all five river catchments.

4.1.2 Differences to 20-50-year precipitation events

By construction, the accumulated daily precipitation amounts for LEPE are significantly smaller than for MEPE, as shown
in Fig. 3b for the Danube catchment. Over the entire catchment, the MEPE composite indicates higher precipitation amounts
and most of these differences are statistically significant. The LEPE composite, which is displayed as black contours, shows
a similar spatial pattern as the MEPE composite with high precipitation amounts within the catchment and a maximum over
the northern part of the Alps. However, MEPE are also associated with significantly higher precipitation rates over southeast
Germany, the Czech Republic as well as around the eastern parts of the Alps. In some regions in the western Alps and eastern
Europe, significantly more precipitation occurs during LEPE. Also in the other river catchments, the spatial patterns of the
LEPE composites are similar to the corresponding MEPE.

A comparison of the temporal occurrence and sub-daily variability of LEPE illustrates a lot of similarities to the 100-year events. The monthly frequencies of LEPE (Fig. 4b) indicate a similar seasonality as for MEPE. LEPE occur most frequently during the extended summer as well, mainly from May to October with a maximum frequency during June, July and August in all river catchments. However, especially over the Rhine catchment, a few events also occur during the other seasons. Hence, although the seasonality of LEPE is less well-defined, there is no shift in the maximum frequency towards other months compared to MEPE.

Also the sub-daily variability of precipitation during LEPE is similar to MEPE (see again Supplementary Fig. S4). The precipitation differences between MEPE and LEPE are similar in all six-hourly sub-periods, indicating that the differences between the events cannot be explained by either differences in peak intensity or persistence alone. The same is true for the other river catchments, only the tendency towards larger differences between six-hourly intensities during MEPE observed for the Weser/Ems and Elbe catchments is less pronounced for LEPE.

4.2 Atmospheric conditions associated with extreme events

4.2.1 100-year precipitation events

In order to characterise the atmospheric conditions associated with 100-year precipitation events, composites of various fields 12 hours after the start of daily MEPE over the Danube catchments are shown in Fig. 5. The temporal evolution of the geopotential height composites prior to the events is shown in Fig. 6. The geopotential height composite at 500 hPa (Fig. 5a) indicates a negative anomaly over Central Europe with its center southeast of the Danube catchment and the Alps, which has the form of an upper-level cut-off low. Similar cut-off low anomalies are found for the other river catchments, with the low pressure center typically located slightly east of the respective catchment (see Supplementary Fig. S5). The additional southward shift to the southern side of the Alps observed for the Danube catchment thus is slightly exceptional. In addition, positive geopotential height anomalies are located over the North Atlantic as well as over Eastern Europe (see again Fig. 5a). The presence of such ridges may lead to a quasi-stationary situation in which the cut-off low is prevented from moving farther east. In the sea level pressure composite for the Danube catchment (contours in Fig. 5a), an extended area of relatively low pressure covers large parts of Central and Eastern Europe, with the low pressure center being located close to and slightly east of the center of the upper-level cut-off low, which is a configuration conductive to baroclinic cyclone growth. An area of high pressure is found over the North Atlantic, underneath the 500 hPa ridge.

The upper-level cut-off low is also visible as positive potential vorticity (PV) anomaly on the 320 K isentrope (Fig. 5b). The center of the PV cut-off is shifted slightly southeastward compared to the center of the geopotential height anomaly at 500 hPa. Such stratospheric PV cut-offs or streamers are created by upper-level Rossby wave breaking (Grams et al., 2011) and have been shown to be often associated with extreme precipitation events in Europe (Martius et al., 2008). Also for the present case of MEPE in the Danube catchment, the composite temporal evolution of the geopotential height field at 500 hPa (Fig. 6) indicates that the cut-off low develops from a trough located over northwestern Europe 24 hours before the event (Fig. 6a). Subsequently, Rossby wave breaking is likely associated with the separation of the negative geopotential height anomaly from
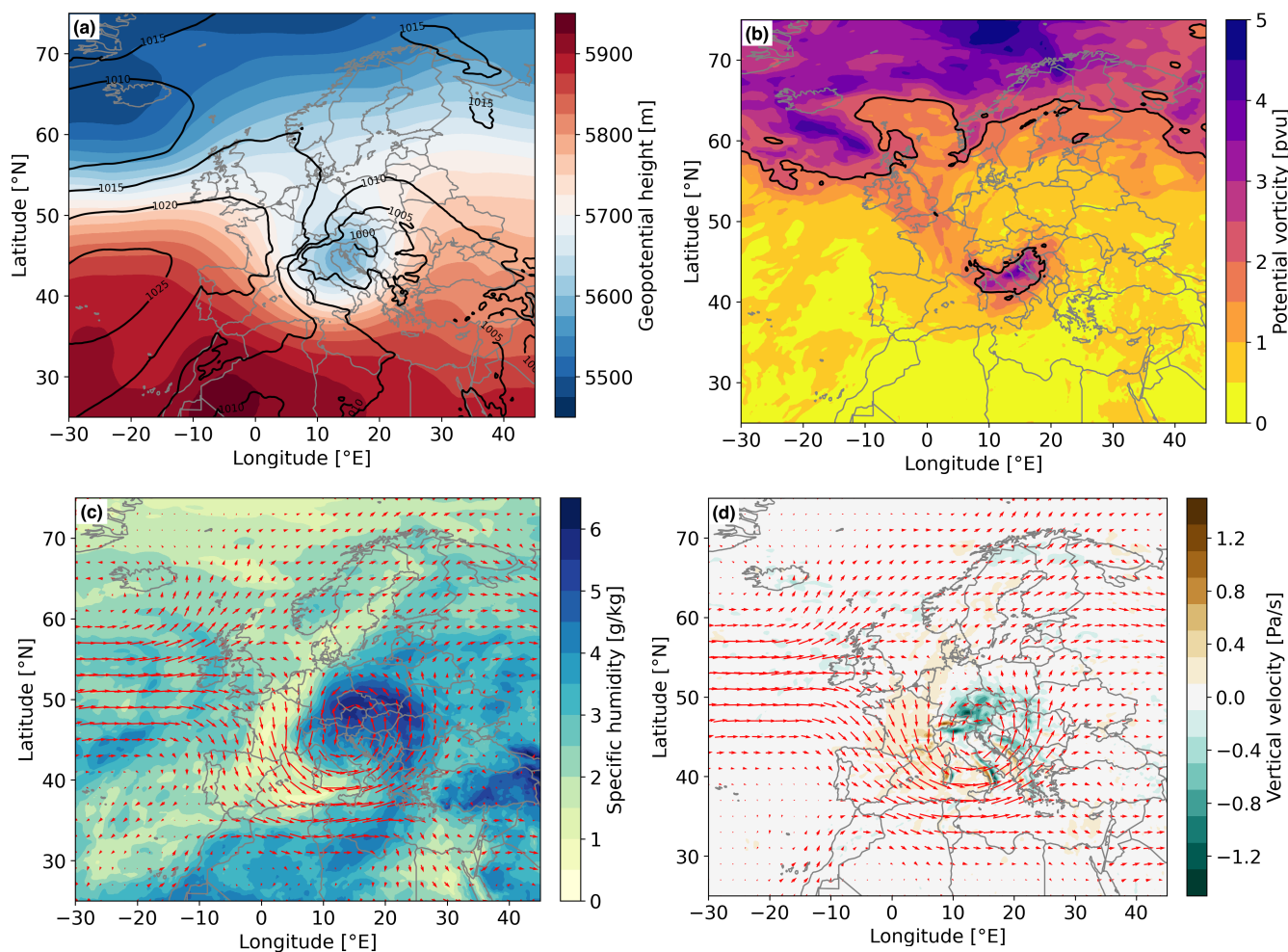
Figure 5. Composites of **(a)** geopotential height at 500 hPa (colour shading) and sea level pressure (contours), **(b)** potential vorticity at 320 K, with the 2 pvu contour is indicated in black, **(c)** specific humidity (colour shading) and horizontal wind (red arrows) at 700 hPa as well as **(d)** vertical velocity (colour shading) and horizontal wind (red arrows) at 500 hPa, for all MEPE over the Danube catchment, 12 hours after the start of the daily extreme events.

375   the main northern region of low geopotential (high PV) and its southeastward displacement and slowdown south of the Danube catchment (Fig. 6b-d). The formation of the cut-off is associated with an intensification of the upstream and downstream ridges as well as surface cyclogenesis (see also section 4.3). MEPE in the other catchments follow a similar development, with the composite trajectory of the upper-level cut-off low and the location of surface cyclogenesis slightly displaced towards the respective catchment region (not shown).

380   The configuration of low pressure over Central Europe and high pressure over the North Atlantic and Eastern Europe is associated with northwesterly winds over Western Europe, westerly winds over the Mediterranean and southerly winds over
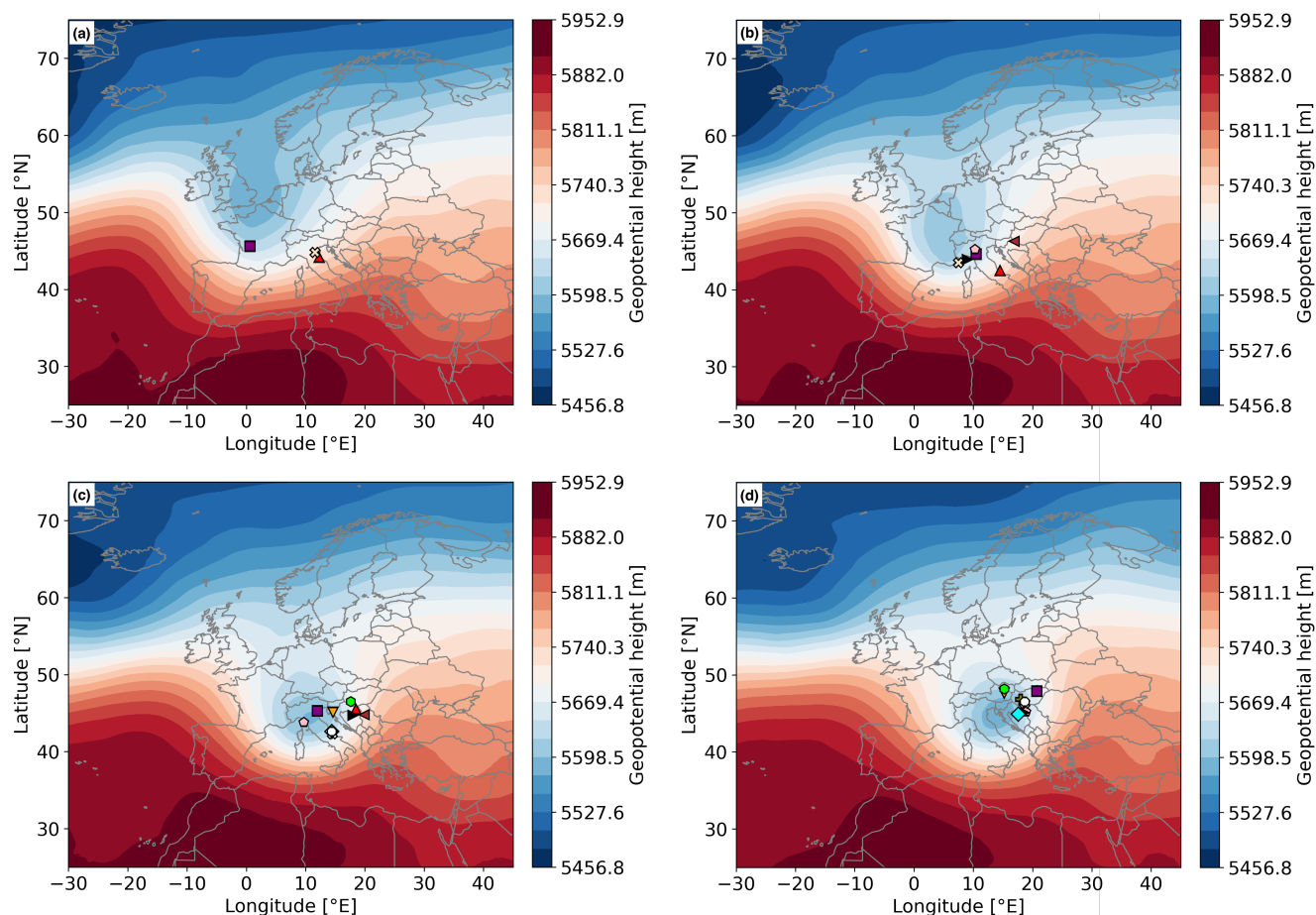
Figure 6. Composites of the geopotential height at 500 hPa for all MEPE over the Danube catchment **(a)** 24 h before the event, **(b)** 12 h before the event, **(c)** at the beginning of the event as well as **(d)** 12 h after the beginning of the event. The surface cyclone centers (sea level pressure minima) from the cyclone identification and tracking approach are shown as coloured symbols. Since not every cyclone was identified for all time steps, later images show higher numbers of identified cyclone centers.

Eastern Europe in the lower and middle troposphere (see Fig. 5c,d). Such a horizontal wind field facilitates the advection of moist air masses over the eastern Mediterranean and Eastern Europe towards Central Europe (Fig. 5c). In addition to the Mediterranean, continental evapotranspiration can act as an important (and often main) moisture source in such situations, as
385 shown in previous case studies (Grams et al., 2014; Winschall et al., 2014; Sodemann et al., 2009; James et al., 2004). The moist air is transported towards the Danube catchment with northeasterly winds, where strong ascent (Fig. 5d) leads to rainout. Dynamical forcing, evident from positive vorticity advection, plays a role for this lifting in all catchments, but is weakest for the Danube (not shown). In addition, orographic effects can intensify the ascent, in particular in the case of the Danube (and also the Rhine) catchment, when the air masses are transported towards the Alpine ridge from the north. The slow displacement

390 of the cut-off low can lead to continual ascent in the same catchment region and high accumulation of precipitation during the
day of the MEPE.

These composites show the average conditions during all 100-year precipitation events over a river catchment. Although
most of the individual events develop in a similar way as shown in these composites, there are a few exceptions with a different
progression. Two events over the Danube catchment are characterised by an upper-level low that moves north of the Alps, but a
395 surface cyclone also developing east of the catchment. One event over the Weser/Ems catchment results from a small northward
moving surface cyclone at the eastern flank of a large upper-level trough over the British Isles and the North Atlantic. Although
the cyclone does not strongly intensify, it facilitates the transport of warm and moist air masses from the south towards the
river catchment. During two events over the Elbe catchment, a large upper-level cut-off low over southeastern Europe moves
northward to Poland in combination with the intensification of a surface cyclone to the north and moisture transport also
400 from the Black Sea region. Two other events are characterised by an omega blocking centered over Scandinavia and a large
ridge over the catchment in between two lows over the British Isles and Eastern Europe, but no clear surface cyclone. Moist
air masses are transported from Southern to Central Europe ahead of the western low pressure system, and lifting over the
catchment is associated with a near-surface convergence zone. Additionally, an event over the Oder catchment is linked to a
"high over low" blocking system over the British Isles and a convergence zone over the catchment as well as three events over
405 the Rhine catchment that are characterised by a positive, upper-level geopotential height anomaly over Eastern Europe with an
upper-level trough that slowly moves from the British Isles towards the catchment while surface cyclones develop north of the
Alps.

4.2.2 Differences to 20-50-year precipitation events

The previous section has shown that the atmospheric conditions during 100-year precipitation events are often similar between
410 the different river catchments. In this section, differences between 100-year and more moderate, 20-50-year precipitation events
are identified through differences between MEPE and LEPE composites. Figures 7 and 8 show such composite differences for
the Danube and Elbe catchments, respectively, as different mechanisms distinguish MEPE over these catchments.

LEPE over the Danube catchment are associated with a similar upper-level pattern as MEPE, with an upper-level cut-off low
located over Central Europe centered slightly south of the river catchment in combination with ridges over the North Atlantic
415 and Eastern Europe (Fig. 7a). Also the surface pressure configuration is similar with a large area of low pressure over Eastern
Europe and high pressure over the North Atlantic (Fig. 7b). However, MEPE are characterised by a significantly intensified low
pressure anomaly at 500 hPa that also extends further south compared to LEPE. In addition, the surface pressure is significantly
lower over large parts of Central and Eastern Europe. Pressure is also lower around Iceland both at the surface and in the middle
troposphere. The intensified cut-off low and associated cyclonic circulation during MEPE is associated with intensified cold air
420 advection, bringing colder air masses over the Mediterranean Sea along the southern flank of the cut-off low (Fig. 7c). Over the
Danube catchment itself, no significant temperature difference occurs, but still the temperature is slightly higher during MEPE
northeast of the catchment. There is also no particular increase of the moisture content in the lower troposphere over most parts
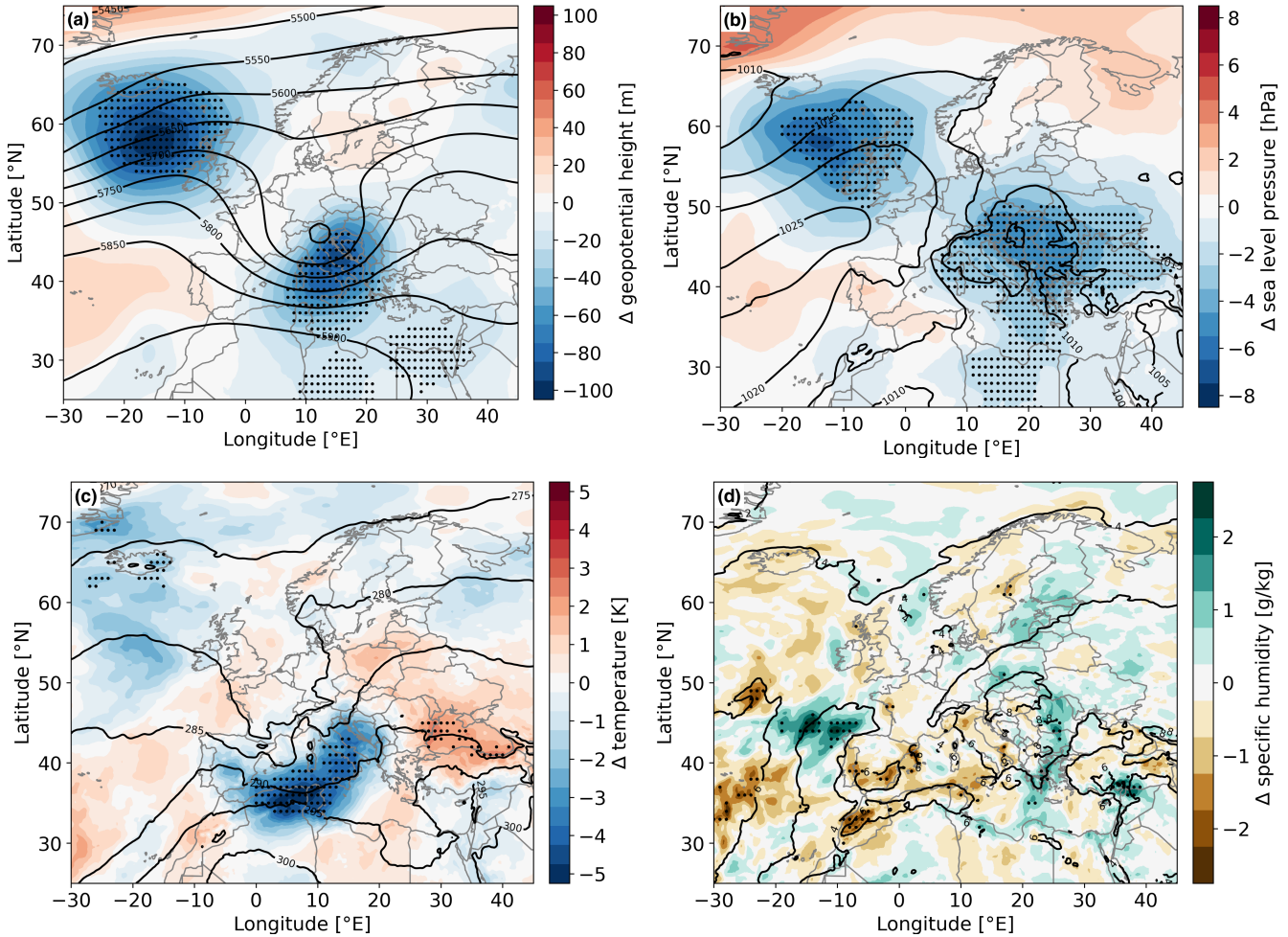
Figure 7. Differences between the composites of MEPE and LEPE over the Danube catchment for **(a)** geopotential height at 500 hPa, **(b)** sea level pressure, **(c)** temperature at 850 hPa as well as **(d)** specific humidity at 850 hPa. Positive (negative) values indicate higher (lower) values in the MEPE composite. Significant differences are marked by black dots. The LEPE composites are shown as black contours.

of Central and Eastern Europe, although some areas are characterised by minor increases during MEPE (Fig. 7d). Figures 7a and b thus clearly show that dynamical mechanisms such as an intensified cut-off low at 500 hPa and intensified low pressure
425 systems at the surface play a more important role than thermodynamic mechanisms (larger temperature or moisture content in the lower troposphere) in distinguishing 100-year extreme precipitation events from more moderate extreme events. Similar results are found for the Oder catchment (not shown), where, in addition, also the 500 hPa ridge over the North Atlantic is slightly intensified during MEPE. Furthermore, the lower-tropospheric moisture content is significantly reduced during MEPE over several areas of Central Europe.
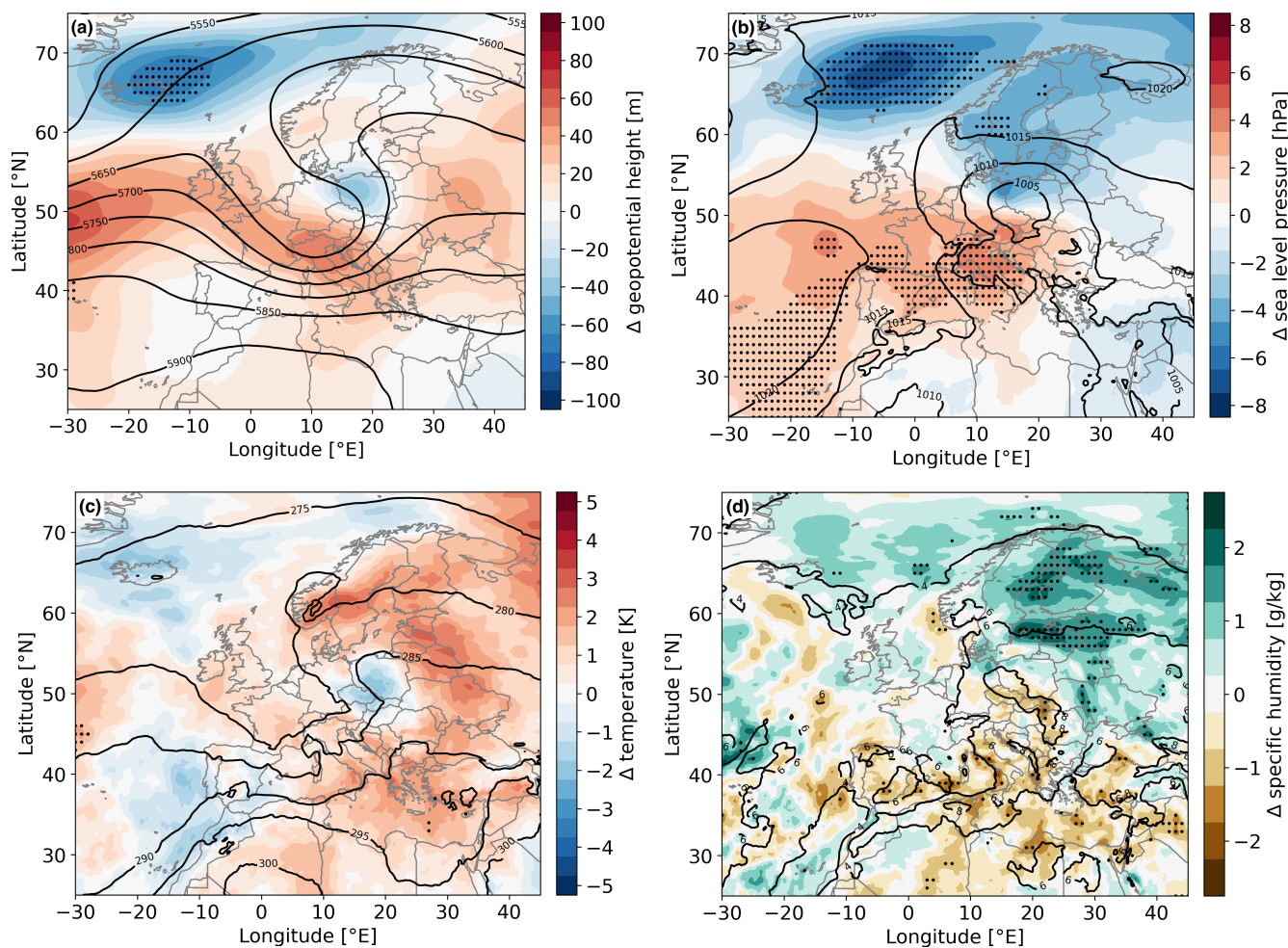
Figure 8. Same as in Fig. 7, but for events over the Elbe catchment.

430   Not in all catchments MEPE are characterised by intensified circulation anomalies in comparison to LEPE. In order to demonstrate different intensification mechanisms, composite differences between MEPE and LEPE are shown in Fig. 8 for the Elbe catchments. MEPE over this catchment are rather associated with a slight northeastward shift of the 500 hPa low towards the east of the catchment instead of a clear intensification (Fig. 8a). Over the North Atlantic, the height of the 500 hPa surface is lower over Iceland and the ridge west of Ireland is slightly intensified during MEPE. Similar results are found for sea level

435   pressure (Fig. 8b). The local sea level pressure minimum over Eastern Europe is shifted northeastwards during MEPE rather than being intensified compared to LEPE. On a larger scale, sea level pressure values are generally lower over the northern part of the domain, but higher in the southwest during MEPE. On the contrary, as opposed to the Danube catchment, the lower-tropospheric temperature over large parts of Eastern Europe is higher during MEPE compared to LEPE over the Elbe catchment, even though this difference is not statistically significant (Fig. 8c). The local cold anomaly over the Czech Republic and

440   southern Poland is caused by the extreme precipitation event (e.g., due to cloud radiative cooling) and is not visible in the hours before the event (not shown). These generally higher temperatures go along with significantly increased lower-tropospheric moisture content, in particular in the region northeast of the sea level pressure minimum (Fig. 8d). This moisture can then be transported towards the Elbe catchment by the cyclonic circulation. In summary, more favourable thermodynamic conditions, in particular a higher atmospheric moisture content, thus distinguish MEPE over the Elbe catchment. The circulation anomalies

445   associated with these events are spatially shifted rather than intensified compared to LEPE. Similar results are obtained for the Rhine catchment (not shown). MEPE over the Rhine catchment are characterised by a southward shift of the mid-level and surface low pressure anomalies in combination with a significant intensification of an upper-level ridge over Northern and Eastern Europe. Additionally, temperature and lower-tropospheric moisture content are significantly higher during MEPE over most of Eastern Europe.

450   In the Weser/Ems catchment, both dynamic and thermodynamic mechanisms play a role for the differences between MEPE and LEPE (not shown). The negative 500 hPa geopotential height anomaly is slightly enhanced and the surface low is significantly intensified during MEPE. Both temperature and lower-tropospheric moisture content are significantly higher over parts of Eastern Europe, but conditions are even drier over large parts of Central and Western Europe.

4.3   Cyclone development

455   The composite method to identify typical atmospheric patterns associated with extreme precipitation events is complemented by an event-based approach to objectively identify and track surface cyclones as described in section 3.5. Cyclones are associates with both MEPE and LEPE at the day of the event and tracks are connected backward in time until cyclone genesis. The positions of the surface cyclone centers associated with MEPE are shown as coloured symbols in Fig. 6, the cyclone frequency during MEPE (taking all grid points within the outermost closed sea level pressure contour surrounding a sea level minimum

460   into account) in Fig. 9a. Most cyclones emerge downstream of the developing cut-off low at 500 hPa (see colour shading in Fig. 6), in an area that is favourable for cyclogenesis, the day before or at the day of the MEPE. Most surface cyclones develop south of the Alps and move in parallel with the mid-tropospheric low along the Alps and towards the east or southeast of the Danube catchment. Such cyclone pathways are represented by the "Vb" type in the categorisation of van Bebber (1891). The cyclone frequency during MEPE has a maximum southeast of the Danube catchment, with values around 80% over northern

465   Croatia and western Hungary (see again Fig. 9a). The cyclone tracking results for MEPE over the Elbe and Oder catchments are similar to the Danube catchment, with cyclones also developing south of the Alps, but also over Eastern Europe, and then moving northwards. Surface cyclones during MEPE over the Rhine catchment rather develop north of the Alps or over the western Mediterranean and track northwards, while those associated with MEPE over the Weser/Ems catchment mainly develop over southern and eastern Germany. Cyclones associated with LEPE typically follow similar pathways as described

470   for MEPE, with only a few exceptions, in all river catchments (not shown). Nevertheless, relative cyclone frequencies during LEPE are smaller than for MEPE (see Table 2 and, for the Danube catchment, Fig. 9b), meaning that a smaller percentage of LEPE events is linked to a tracked surface cyclone. Moreover, also the cyclone intensity, measured here simply by the averaged minimum sea level pressure, is enhanced for MEPE compared to LEPE (see again Table 2). These intensity differences
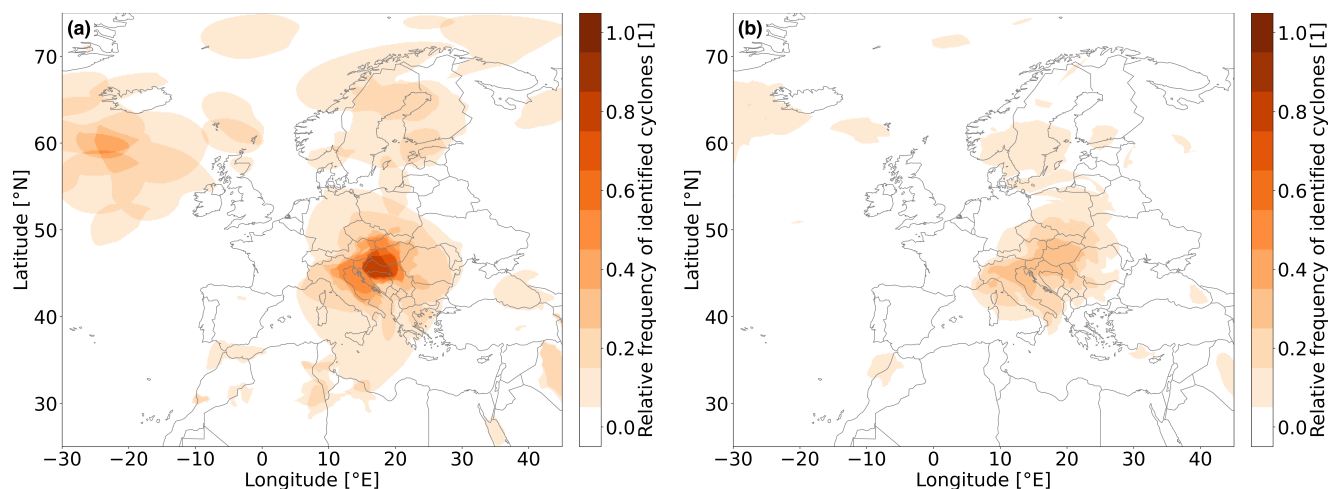
Figure 9. Cyclone frequency at 6 UTC on the day of **(a)** MEPE and **(b)** LEPE over the Danube catchment. All grid points within the outermost closed sea level pressure contour surrounding a sea level minimum are taken into account for the calculation of this frequency, following previous studies (Pfahl, 2014; Wernli and Schwierz, 2006).

Catchments	Cyclone frequency				Mean minimum SLP	
	MEPE		LEPE		MEPE	LEPE
Rhine	11/13	(84.6%)	27/42	(64.3%)	999.0 hPa	1002.5 hPa
Weser/Ems	10/10	(100.0%)	20/29	(69.0%)	**992.4 hPa**	**999.6 hPa**
Elbe	10/11	(90.9%)	30/38	(79.0%)	995.3 hPa	996.6 hPa
Oder	12/13	(92.3%)	24/36	(66.7%)	**992.8 hPa**	**999.7 hPa**
Danube	11/13	(84.6%)	21/41	(51.2%)	995.8 hPa	999.5 hPa

Table 2. Absolute and relative cyclone frequencies as well as mean cyclone intensities, measured through the minimum sea level pressure, of cyclones associated with MEPE and LEPE. Bold SLP indicate significant differences on a significance level of 0.05.

are larger for the Weser/Ems, Oder and Danube catchments, and even statistically significant for the former two, compared to
475 Rhine and Elbe. This is consistent with the result from the composite analysis that dynamical factors distinguish MEPE from LEPE in the former three catchments (see section 4.2.2).

In addition to the cyclone pathway and intensity, its velocity may be an important factor for extreme precipitation, as slower moving systems can lead to larger precipitation accumulation at a specific location. In order to analyse cyclone velocities, Fig. 10 shows the travelled distances of tracked cyclones in 6-hourly intervals for MEPE (in red) and LEPE (in blue). Only at
480 the day of the events and the previous day, reasonable distributions can be produced as the number of identified cyclones is too low during earlier periods (see grey bars in Fig. 10). In general, cyclones tend to decelerate at the day of the event compared to the previous day, which is consistent with the hypothesis that slower moving cyclones can enhance the precipitation amounts in
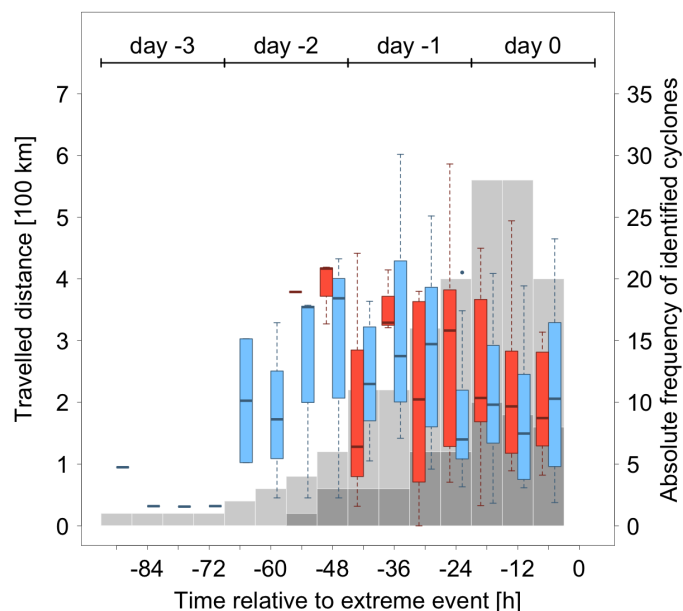
Figure 10. Distributions of travelled distances during 6-hourly time intervals of tracked cyclones during (red) MEPE and (blue) LEPE over the Danube catchment. The grey bars show the absolute cyclone counts at each time step for (dark grey) MEPE and (light grey) LEPE. The time on the x-axis is specified relative to the occurrence of the extreme event, and 0 hours corresponds to the end of the daily event.

the river catchments. However, comparing cyclone velocities between MEPE and LEPE during the day of the extreme events shows that there is a large scatter and no clear difference of the median velocities. Similar results are found for the other river
485   catchments (not shown). Only for the Elbe and Oder catchments, there is a slight tendency towards slower cyclones for MEPE compared to LEPE.

In summary, the results of the cyclone tracking analysis show that extreme precipitation events in the selected river catchments are associated with typical cyclone tracks from the south towards the east of the respective catchment, and with a deceleration of the cyclones during the day of the event. MEPE are linked to higher cyclone frequencies and also more intense
490   cyclones compared to LEPE, in particular in the Oder, Danube and Weser/Ems catchments. However, the cyclones' translation velocities are similar for MEPE and LEPE and thus do not allow distinguishing 100-year from less extreme precipitation events.

5   Discussion and conclusion

The aim of this study has been to robustly investigate the atmospheric processes during 100-year precipitation events in large
495   Central European river catchments and their differences compared to less extreme events. A better understanding of these high-impact events may be instrumental to provide more accurate forecasts of river floods and reduce uncertainties in projections of their potential future changes. To perform such a robust process analysis, we use a large data set of model-generated

daily precipitation fields obtained from the ECMWF operational ensemble weather prediction system following a method introduced by Breivik et al. (2013). Statistical analyses show that the 10th forecast days from these simulations produce quasi-

500 independent precipitation events, in particular with regard to extremes such as annual maxima, and that the intensity distribution of these simulated events lies within the uncertainties obtained from different observational data sets. With the help of extreme value theory, return levels of 100-year and more moderate, 20-50-year extreme precipitation events are determined for each selected river catchment, and the events surpassing these return levels are investigated with regard to the underlying atmospheric conditions.

505 An analysis of the temporal and spatial characteristics of the extreme precipitation events shows that most 100-year events occur during the extended summer June-September, with only a few exceptions in May or October. This corresponds well with historical precipitation extremes (e.g., Grams et al., 2014; Ulbrich et al., 2003) and statistical analyses of rain gauge data (Fischer et al., 2016). More moderate precipitation extremes also peak during the summer season, but may occur during winter in the Rhine and Weser/Ems catchments as well. The spatial distribution of precipitation during the extreme events is influenced

510 by the topography of the catchments, in particular by the orographic effect of the Alps in the Danube and Rhine catchments.

In order to determine the characteristic atmospheric conditions associated with the 100-year precipitation events, a composite analysis is used in combination with a cyclone tracking algorithm. On the day before the events, an upper-level trough is typically located over Western Europe, which slowly moves southeastwards in the direction of the Alps. Rossby wave breaking then leads to the formation of a cut-off low in the middle and upper troposphere that is visible as both a geopotential height

515 and potential vorticity anomaly. Previous studies also emphasised the importance of Rossby wave breaking for European precipitation extremes, in particular on the south side of the Alps (Barton et al., 2016; Martius et al., 2008). The resulting cut-off low can favour the formation of extreme precipitation through its influence on moisture transport, lower-tropospheric destabilisation and dynamical lifting (Schlemmer et al., 2010). The exact pathway and location of the forming cut-off, typically towards the southeast of the specific river catchment, determines where the heavy precipitation event occurs. During the day of

520 the event, the upper-level cut-off low becomes quasi-stationary, also associated with the formation of high pressure anomalies upstream over the North Atlantic and downstream over Eastern Europe. Surface cyclogenesis regularly occurs east of the mid-tropospheric cut-off shortly before or during the extreme precipitation event. Cyclone pathways often, but not in all cases and for all catchments, resemble the classical "Vb" track (van Bebber, 1891), which has been associated also with many historical events (Hofstätter et al., 2018; Messmer et al., 2015; Grams et al., 2014; Bissolli et al., 2011; Mudelsee et al., 2004; Ulbrich

525 et al., 2003). The involved cyclones are not necessarily very intense, consistent with previous findings (Pfahl and Wernli, 2012), but, in accordance with the upper-level anomalies, move slowly and thus lead to high precipitation accumulation in the catchment. The spatial configuration with a cyclone typically located to the southeast of the affected catchment is again consistent with similar configurations found for less extreme precipitation events (Pfahl, 2014). It leads to moisture transport from the south around the cyclone centers and then towards the catchment with northerly or northeasterly winds. This is

530 especially relevant for the Danube and Rhine catchments as a northerly flow towards the Alps enforces orographic precipitation enhancement. Previous case studies have shown that, during such situations, typically various moisture sources contribute to the precipitation, with evapotranspiration from the land surface often playing the dominant role (Krug et al., 2022; Grams et al.,

2014; Winschall et al., 2014). The important role of moisture transport in particular for orographic precipitation associated with European floods has already been recognised in previous studies (Gvoždíková and Müller, 2021; Froidevaux and Martius, 535   2016).

To identify the mechanism that distinguish the very extreme, 100-year precipitation events (MEPE), they are compared to a sample of less extreme events with return periods between 20 and 50 years (LEPE). The general synoptic-scale patterns associated with LEPE are similar to MEPE, with an upper-level trough over Western Europe on the day before the event that often develops into a cut-off low, going along with surface cyclogenesis slightly downstream. The specific differences between 540   MEPE and LEPE depend on the river catchment. On the one hand, differences in dynamical processes are most important for the Danube and Oder catchments. In particular, the cut-off low is intensified, surface cyclogenesis occurs more regularly and the surface cyclones are also more intense during MEPE compared to LEPE. This is expected to enhance moisture transport towards and dynamical forcing for ascent in the catchments, resulting in stronger precipitation. These results are in slight contrast to the findings of Pfahl and Wernli (2012), who did not detect differences in the intensity of cyclones associated 545   with extreme precipitation (albeit less extreme than the events studied here) in Central Europe. However, there are no clear differences between the translation velocities of cyclones associated with MEPE and LEPE. On the other hand, MEPE in the Elbe and Rhine catchments differ from LEPE mainly due to significantly higher temperature and lower-tropospheric moisture content over large areas east and northeast of the river catchments. No pronounced differences in the strength of cyclones and cut-off lows are found for these catchments. The enhanced precipitation during MEPE can thus mainly be explained by higher 550   moisture content in the air masses transported towards the catchments. Finally, in the Weser/Ems catchment both stronger circulation anomalies and higher moisture content distinguish MEPE from LEPE.

In this study, the first systematic analysis is presented of very extreme 100-year large-scale precipitation events in Central Europe that goes beyond case studies. As the observational record is too short, we have to rely on simulated events, but a comparison to observations has shown that precipitation intensities are realistically represented in the applied ensemble 555   prediction model. In future research, the approach may be used also for multi-day events, which have a high potential to cause flooding as well, with the help of more recent ECMWF forecast data extending beyond lead times of 10 days. Additionally, the method may be applied to other regions, as the data set is available for the entire globe.

Data availability. The operational IFS ensemble forecast data from ECMWF can be obtained from https://apps.ecmwf.int/archive-catalogue/ ?type=cf&class=od&stream=enfo&expver=1 and https://apps.ecmwf.int/archive-catalogue/?type=pf&class=od&stream=enfo&expver=1 (last 560   access: 25th April 2022). The user's affiliation needs to belong to an ECMWF member state. The observational data set REGEN is freely available from https://geonetwork.nci.org.au/geonetwork/srv/eng/catalog.search#/metadata/f8555_9260_4736_9502 (last access: 25th April 2022) (Contractor et al., 2020). The observational data HYRAS can be accessed from https://gdk.gdi-de.org/geonetwork/srv/api/records/de. dwd.hydromet.hyras.daily.info.status (last access: 25th April 2022). The observational E-OBS data can be downloaded from the ECA&D project via https://www.ecad.eu/download/ensembles/download.php (last access: 25th April 2022).

Author contributions. FR performed the analysis, produced the figures and drafted the manuscript. Both authors designed the study, discussed results and edited the manuscript.

Competing interests. SP is a member of the editorial board of Weather and Climate Dynamics. The authors have no other competing interests to declare.

Acknowledgements. This study has been funded by the German Ministry of Education and Research (Bundesministerium für Bildung und Forschung, BMBF) in its strategy "Research for Sustainability" (FONA) in the framework of the "ClimXtreme" program, sub-project A2 (MExRain, grant number 01LP1901C). The German Meteorological Service DWD and ECMWF are acknowledged for providing the operational IFS model data. This work used resources of the Deutsches Klimarechenzentrum (DKRZ) which is granted by its Scientific Steering Committee (WLA) under project ID bb1152. We are greatful to Heini Wernli (ETH Zurich) for his helpful comments on the event process analysis, to Felix Fauer and Henning Rust (both Freie Universität Berlin) for their helpful comments on the statistical analysis, to Hendrik Feldmann (Karlsruhe Institute of Technology) for the hint to possible observational data sets as well as to all colleagues of the "ClimXtreme" Module D for their technical assistance.

References

Barredo, J. I.: Major flood disasters in Europe: 1950–2005, Natural Hazards, 42, 125–148, 2007.

Barton, Y., Giannakaki, P., Von Waldow, H., Chevalier, C., Pfahl, S., and Martius, O.: Clustering of regional-scale extreme precipitation events in southern Switzerland, Monthly Weather Review, 144, 347–369, 2016.

Benjamini, Y. and Hochberg, Y.: Controlling the false discovery rate: a practical and powerful approach to multiple testing, Journal of the Royal statistical society: series B (Methodological), 57, 289–300, 1995.

Bissolli, P., Friedrich, K., Rapp, J., and Ziese, M.: Flooding in eastern central Europe in May 2010–reasons, evolution and climatological assessment, Weather, 66, 147–153, 2011.

Blöschl, G., Nester, T., Komma, J., Parajka, J., and Perdigão, R. A.: The June 2013 flood in the Upper Danube Basin, and comparisons with the 2002, 1954 and 1899 floods, Hydrology and Earth System Sciences, 17, 5197–5212, 2013.

Breivik, Ø., Aarnes, O. J., Bidlot, J.-R., Carrasco, A., and Saetra, Ø.: Wave extremes in the northeast Atlantic from ensemble forecasts, Journal of Climate, 26, 7525–7540, 2013.

Coles, S., Bawa, J., Trenner, L., and Dorazio, P.: An introduction to statistical modeling of extreme values, vol. 208, Springer, 2001.

Contractor, S., Donat, M. G., Alexander, L. V., Ziese, M., Meyer-Christoffer, A., Schneider, U., Rustemeier, E., Becker, A., Durre, I., and Vose, R. S.: Rainfall Estimates on a Gridded Network (REGEN)–a global land-based gridded dataset of daily precipitation from 1950 to 2016, Hydrology and Earth System Sciences, 24, 919–943, 2020.

Cornes, R. C., van der Schrier, G., van den Besselaar, E. J., and Jones, P. D.: An ensemble version of the E-OBS temperature and precipitation data sets, Journal of Geophysical Research: Atmospheres, 123, 9391–9409, 2018.

Donat, M., Alexander, L. V., Yang, H., Durre, I., Vose, R., Dunn, R. J., Willett, K. M., Aguilar, E., Brunet, M., Caesar, J., et al.: Updated analyses of temperature and precipitation extreme indices since the beginning of the twentieth century: The HadEX2 dataset, Journal of Geophysical Research: Atmospheres, 118, 2098–2118, 2013.

Engel, H.: The flood events of 1993/1994 and 1995 in the Rhine River basin, IAHS Publications-Series of Proceedings and Reports-Intern Assoc Hydrological Sciences, 239, 21–32, 1997.

Engel, H.: The flood event 2002 in the Elbe river basin, causes of the flood, its course, statistical assessment and flood damages, La Houille Blanche, 90, 33–36, 2004.

Fischer, E. M., Beyerle, U., and Knutti, R.: Robust spatially aggregated projections of climate extremes, Nature Climate Change, 3, 1033–1038, 2013.

Fischer, M., Rust, H. W., and Ulbrich, U.: Seasonal cycle in German daily precipitation extremes, Meteorologische Zeitschrift, pp. 1–11, 2016.

Froidevaux, P. and Martius, O.: Exceptional integrated vapour transport toward orography: an important precursor to severe floods in Switzerland, Quarterly Journal of the Royal Meteorological Society, 142, 1997–2012, 2016.

Grams, C. M., Wernli, H., Böttcher, M., Čampa, J., Corsmeier, U., Jones, S. C., Keller, J. H., Lenz, C.-J., and Wiegand, L.: The key role of diabatic processes in modifying the upper-tropospheric wave guide: a North Atlantic case-study, Quarterly Journal of the Royal Meteorological Society, 137, 2174–2193, 2011.

Grams, C. M., Binder, H., Pfahl, S., Piaget, N., and Wernli, H.: Atmospheric processes triggering the central European floods in June 2013, Natural Hazards and Earth System Sciences, 14, 1691–1702, 2014.

Gvoždíková, B. and Müller, M.: Moisture fluxes conducive to central European extreme precipitation events, Atmospheric Research, 248, 105 182, 2021.

615 Hammond, M. J., Chen, A. S., Djordjević, S., Butler, D., and Mark, O.: Urban flood impact assessment: A state-of-the-art review, Urban Water Journal, 12, 14–29, 2015.

Hofstätter, M., Lexer, A., Homann, M., and Blöschl, G.: Large-scale heavy precipitation over central Europe and the role of atmospheric cyclone track types, International Journal of Climatology, 38, e497–e517, 2018.

James, P., Stohl, A., Spichtinger, N., Eckhardt, S., and Forster, C.: Climatological aspects of the extreme European rainfall of August 2002

620 and a trajectory method for estimating the associated evaporative source regions, Natural Hazards and Earth System Sciences, 4, 733–746, 2004.

Kenyon, J. and Hegerl, G. C.: Influence of modes of climate variability on global precipitation extremes, Journal of Climate, 23, 6248–6262, 2010.

Kreibich, H., Bubeck, P., Kunz, M., Mahlke, H., Parolai, S., Khazai, B., Daniell, J., Lakes, T., and Schröter, K.: A review of multiple natural

625 hazards and risks in Germany, Natural Hazards, 74, 2279–2304, 2014.

Krug, A., Aemisegger, F., Sprenger, M., and Ahrens, B.: Moisture sources of heavy precipitation in Central Europe in synoptic situations with Vb-cyclones, Climate Dynamics, pp. 1–19, 2022.

Maraun, D., Osborn, T. J., and Rust, H. W.: The influence of synoptic airflow on UK daily precipitation extremes. Part I: Observed spatio-temporal relationships, Climate Dynamics, 36, 261–275, 2011.

630 Martius, O., Schwierz, C., and Davies, H.: Far-upstream precursors of heavy precipitation events on the Alpine south-side, Quarterly Journal of the Royal Meteorological Society: A journal of the atmospheric sciences, applied meteorology and physical oceanography, 134, 417–428, 2008.

Merz, B., Elmer, F., Kunz, M., Mühr, B., Schröter, K., and Uhlemann-Elmer, S.: The extreme flood in June 2013 in Germany, La Houille Blanche, pp. 5–10, 2014.

635 Messmer, M., Gómez-Navarro, J. J., and Raible, C. C.: Climatology of Vb cyclones, physical mechanisms and their impact on extreme precipitation over Central Europe, Earth system dynamics, 6, 541–553, 2015.

Molteni, F., Buizza, R., Palmer, T. N., and Petroliagis, T.: The ECMWF ensemble prediction system: Methodology and validation, Quarterly journal of the royal meteorological society, 122, 73–119, 1996.

Mudelsee, M., Börngen, M., Tetzlaff, G., and Grünewald, U.: Extreme floods in central Europe over the past 500 years: Role of cyclone

640 pathway "Zugstrasse Vb", Journal of Geophysical Research: Atmospheres, 109, 2004.

Mueller, M.: Damages of the Elbe flood 2002 in Germany-a review, in: EGS-AGU-EUG Joint Assembly, p. 12992, 2003.

Munich RE: Hurricanes, cold waves, tornadoes: Weather disasters in USA dominate natural disaster losses in 2021, https://www.munichre. com/en/company/media-relations/media-information-and-corporate-news/media-information/2022/natural-disaster-losses-2021.html, 2022.

645 O'Gorman, P. A. and Schneider, T.: The physical basis for increases in precipitation extremes in simulations of 21st-century climate change, Proceedings of the National Academy of Sciences, 106, 14 773–14 777, 2009.

Pendergrass, A. G. and Hartmann, D. L.: Changes in the distribution of rain frequency and intensity in response to global warming, Journal of Climate, 27, 8372–8383, 2014.

Pfahl, S.: Characterising the relationship between weather extremes in Europe and synoptic circulation features, Natural Hazards and Earth

650 System Sciences, 14, 1461–1475, 2014.

Pfahl, S. and Wernli, H.: Quantifying the relevance of cyclones for precipitation extremes, Journal of Climate, 25, 6770–6780, 2012.

Rauthe, M., Steiner, H., Riediger, U., Mazurkiewicz, A., and Gratzki, A.: A Central European precipitation climatology–Part I: Generation and validation of a high-resolution gridded daily data set (HYRAS), Meteorol. Z, 22, 235–256, 2013.

Re, M.: Naturkatastrophen in Deutschland: Schadenerfahrungen und Schadenpotentiale, Publication of the Munich Re, Order Number, 1999.

655 Schlemmer, L., Martius, O., Sprenger, M., Schwierz, C., and Twitchett, A.: Disentangling the forcing mechanisms of a heavy precipitation event along the Alpine south side using potential vorticity inversion, Monthly weather review, 138, 2336–2353, 2010.

Sillmann, J., Kharin, V., Zhang, X., Zwiers, F., and Bronaugh, D.: Climate extremes indices in the CMIP5 multimodel ensemble: Part 1. Model evaluation in the present climate, Journal of Geophysical Research: Atmospheres, 118, 1716–1733, 2013.

Sodemann, H., Wernli, H., and Schwierz, C.: Sources of water vapour contributing to the Elbe flood in August 2002—A tagging study in a
660 mesoscale model, Quarterly Journal of the Royal Meteorological Society: A journal of the atmospheric sciences, applied meteorology and physical oceanography, 135, 205–223, 2009.

Sprenger, M., Fragkoulidis, G., Binder, H., Croci-Maspoli, M., Graf, P., Grams, C. M., Knippertz, P., Madonna, E., Schemm, S., Škerlak, B., et al.: Global climatologies of Eulerian and Lagrangian flow features based on ERA-Interim, Bulletin of the American Meteorological Society, 98, 1739–1748, 2017.

665 Statista: Teuerste Naturkatastrophen für die weltweite Versicherungswirtschaft im Jahr 2021 nach Gesamtschaden und versichertem Schaden, https://de.statista.com/statistik/daten/studie/195502/umfrage/ groesste-naturkatastrophen-weltweit-nach-gesamt-und-versicherungsschaden/#professional, 2022.

Stephenson, A. G.: evd: Extreme Value Distributions, R News, 2, 0, https://CRAN.R-project.org/doc/Rnews/, 2002.

Szalińska, W., Otop, I., and Tokarczyk, T.: Precipitation extremes during flooding in the Odra River Basin in May-June 2010, Meteorology
670 Hydrology and Water Management. Research and Operational Applications, 2, 2014.

Ulbrich, U., Brücher, T., Fink, A. H., Leckebusch, G. C., Krüger, A., and Pinto, J. G.: The central European floods of August 2002: Part 2-Synoptic causes and considerations with respect to climatic change, Weather, 58, 434–442, 2003.

van Bebber, W.: Die Zugstrassen der barometrischen Minima nach den Bahnenkarten der deutschen Seewarte für den Zeitraum 1875-1890, 8, Meteorologische Zeitschrift, 1891.

675 Ventura, V., Paciorek, C. J., and Risbey, J. S.: Controlling the proportion of falsely rejected hypotheses when conducting multiple tests with climatological data, Journal of Climate, 17, 4343–4356, 2004.

Wasserstraßen- und Schifffahrtsverwaltung des Bundes: Gewässereinzugsgebiete Deutschland (WMS), https://www.gdws.wsv.bund.de/DE/ service/karten/02_Geodatendienste_Geoanwendungen/01_Geodatendienste_NEU/Geodatendienste_node.html#doc1232544bodyText7, 2022.

680 Wernli, H. and Schwierz, C.: Surface cyclones in the ERA-40 dataset (1958–2001). Part I: Novel identification method and global climatology, Journal of the atmospheric sciences, 63, 2486–2507, 2006.

Winschall, A., Pfahl, S., Sodemann, H., and Wernli, H.: Comparison of Eulerian and Lagrangian moisture source diagnostics–the flood event in eastern Europe in May 2010, Atmospheric Chemistry and Physics, 14, 6605–6619, 2014.